

2. Radiative rare B decays

A. Ali and M. Misiak

The transitions $b \rightarrow s(d)\gamma$ and $b \rightarrow s(d)\ell^+\ell^-$ receive sizable contributions from loops involving the top quark (Fig. 6.9). Their dependence on V_{ts} and V_{td} may be used to test unitarity of the CKM matrix and to overconstrain the Wolfenstein parameters $\bar{\rho}$ and $\bar{\eta}$. The considered transitions manifest themselves in exclusive \bar{B} -meson decays like $\bar{B} \rightarrow K^*\gamma$, $\bar{B} \rightarrow K^*\ell^+\ell^-$, $\bar{B} \rightarrow \rho\gamma$ and $\bar{B} \rightarrow \rho\ell^+\ell^-$. The corresponding inclusive decays $\bar{B} \rightarrow X_{s(d)}\gamma$ and $\bar{B} \rightarrow X_{s(d)}\ell^+\ell^-$ are experimentally more challenging, but the theoretical predictions are significantly more accurate, thanks to the use of OPE and HQET. The exclusive processes remain interesting due to possible new physics effects in observables other than just the total branching ratios (photon polarization, isospin- and CP-asymmetries), as well as due to information they provide on non-perturbative form-factors. This information is particularly required in analyzing exclusive modes generated by the $b \rightarrow d\gamma$ transition, in which case there is little hope for an inclusive measurement.

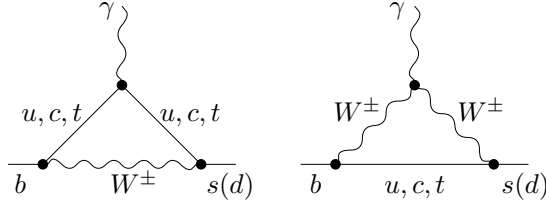


Fig. 6.9: Leading-order Feynman diagrams for $b \rightarrow s(d)\gamma$ in the SM.

In this section we discuss briefly the generic features of the CKM phenomenology in the considered rare B-decays. The transitions $b \rightarrow s\gamma$ and $b \rightarrow s\ell^+\ell^-$ involve the CKM matrix elements from the second and third column of this matrix, with the unitarity constraint taking the form $\sum_{u,c,t} \lambda_i = 0$, with $\lambda_i = V_{ib}V_{is}^*$. This equation yields a unitarity triangle which is highly squashed, as one of the sides of this triangle $\lambda_u = V_{ub}V_{us}^* \simeq A\lambda^4(\bar{\rho} - i\bar{\eta})$ is doubly Cabibbo suppressed, compared to the other two sides $\lambda_c \simeq -\lambda_t = A\lambda^2 + \dots$. Hence, the transitions $b \rightarrow s\gamma$ and $b \rightarrow s\ell^+\ell^-$ are not expected to yield useful information on the parameters $\bar{\rho}$ and $\bar{\eta}$, which define the apex of the unitarity triangle of current interest (see Chapt. 1). The test of unitarity for the $b \rightarrow s$ transitions in rare B-decays lies in checking the relation $\lambda_t \simeq -\lambda_c$, which holds up to corrections of order λ^2 .

The impact of the decays $b \rightarrow d\gamma$ and $b \rightarrow d\ell^+\ell^-$ on the CKM phenomenology is, however, quite different. These transitions involve the CKM matrix elements in the first and third column, with the unitarity constraints taking the form $\sum_{u,c,t} \xi_i = 0$, with $\xi_i = V_{ib}V_{id}^*$. Now, all three matrix elements are of order λ^3 , with $\xi_u \simeq A\lambda^3(\bar{\rho} - i\bar{\eta})$, $\xi_c \simeq -A\lambda^3$, and $\xi_t \simeq A\lambda^3(1 - \bar{\rho} - i\bar{\eta})$. This equation leads to the same unitarity triangle as studied through the constraints V_{ub}/V_{cb} , ΔM_{B_d} (or $\Delta M_{B_d}/\Delta M_{B_s}$). Hence, the transitions $b \rightarrow d\gamma$ and $b \rightarrow d\ell^+\ell^-$ lead to complementary constraints on the CKM parameters $\bar{\rho}$ and $\bar{\eta}$, as illustrated in the following. Thus, the role of rare B-decays is that they provide complementary constraints on the CKM matrix elements, hence test the CKM unitarity, but they also constrain extensions of the Standard Model, and by that token can act as harbinger of new physics.

A theoretical framework for analyzing the $b \rightarrow s\gamma$ transition is set by the effective interaction Hamiltonian

$$\mathcal{H}_{\text{eff}} = -\frac{4G_F}{\sqrt{2}} V_{ts}^* V_{tb} \sum_{i=1}^8 C_i(\mu) Q_i. \quad (24)$$

The generic structure of the operators Q_i is as follows:

$$Q_i = \begin{cases} (\bar{s}\Gamma_i c)(\bar{c}\Gamma'_i b), & i = 1, 2, \\ (\bar{s}\Gamma_i b) \sum_q (\bar{q}\Gamma'_i q), & i = 3, 4, 5, 6, \quad (q = u, d, s, c, b) \\ \frac{em_b}{16\pi^2} \bar{s}_L \sigma^{\mu\nu} b_R F_{\mu\nu}, & i = 7, \\ \frac{g_s m_b}{16\pi^2} \bar{s}_L \sigma^{\mu\nu} T^a b_R G_{\mu\nu}^a, & i = 8. \end{cases} \quad (25)$$

Here, Γ_i and Γ'_i denote various combinations of the colour and Dirac matrices. Everything that is not important for $b \rightarrow s\gamma$ at the leading order in α_{em} , m_b/m_W , m_s/m_b and V_{ub}/V_{cb} has been neglected in Eq. (24).

Perturbative calculations (see Ref. [28] and refs. therein) are used to find the Wilson coefficients in the $\overline{\text{MS}}$ scheme, at the renormalization scale $\mu_b \sim m_b$

$$C_i(\mu_b) = C_i^{(0)}(\mu_b) + \frac{\alpha_s(\mu_b)}{4\pi} C_i^{(1)}(\mu_b) + \left(\frac{\alpha_s(\mu_b)}{4\pi} \right)^2 C_i^{(2)}(\mu_b) + \dots \quad (26)$$

Here, $C_i^{(n)}(\mu_b)$ depend on α_s only via the ratio $\eta \equiv \alpha_s(\mu_0)/\alpha_s(\mu_b)$, where $\mu_0 \sim m_W$. In the Leading Order (LO) calculations, everything but $C_i^{(0)}(\mu_b)$ is neglected in Eq. (26). At the Next-to-Leading Order (NLO), one takes $C_i^{(1)}(\mu_b)$ into account. The Wilson coefficients contain information on the short-distance QCD effects due to hard gluon exchanges between the quark lines of the leading one-loop electroweak diagrams (Fig. 6.9). Such effects enhance the perturbative branching ratio $\mathcal{B}(b \rightarrow s\gamma)$ by roughly a factor of three [29].

The same formalism applies to $b \rightarrow d\gamma$, too. The corresponding operators Q_i are obtained by replacing $\bar{s} \rightarrow \bar{d}$ in Eq. (25), and by including the u -quark analogues of $Q_{1,2}$. The latter operators are no longer CKM-suppressed. The matching conditions $C_i(\mu_0)$ and the solutions of the RG equations, yielding $C_i(\mu_b)$, coincide with those needed for the process $b \rightarrow s\gamma$.

2.1. Inclusive $\overline{\text{B}} \rightarrow X_{s(d)}\gamma$ decay

The inclusive branching ratio $\mathcal{B}(\overline{\text{B}} \rightarrow X_s \gamma)$ was measured for the first time by CLEO in 1995 [30]. The present world averages

$$\mathcal{B}(\overline{\text{B}} \rightarrow X_s \gamma \ (E_\gamma > 1.6 \text{ GeV})) = (3.28^{+0.41}_{-0.36}) \times 10^{-4}, \quad (27)$$

$$\mathcal{B}(\overline{\text{B}} \rightarrow X_s \gamma \ (E_\gamma > \frac{1}{20} m_b)) = (3.40^{+0.42}_{-0.37}) \times 10^{-4} \quad (28)$$

are found from the following four measurements

$$\mathcal{B}(\overline{\text{B}} \rightarrow X_s \gamma \ (E_\gamma > \frac{1}{20} m_b)) = [3.88 \pm 0.36_{\text{stat}} \pm 0.37_{\text{sys}} \left(\begin{smallmatrix} +0.43 \\ -0.23 \end{smallmatrix} \right)_{\text{theory}}] \times 10^{-4}, \quad (\text{BABAR [31]}),$$

$$\mathcal{B}(\overline{\text{B}} \rightarrow X_s \gamma \ (E_\gamma > \frac{1}{20} m_b)) = [3.21 \pm 0.43_{\text{stat}} \pm 0.27_{\text{sys}} \left(\begin{smallmatrix} +0.18 \\ -0.10 \end{smallmatrix} \right)_{\text{theory}}] \times 10^{-4}, \quad (\text{CLEO [32]}),$$

$$\mathcal{B}(\overline{\text{B}} \rightarrow X_s \gamma \ (E_\gamma > \frac{1}{20} m_b)) = [3.36 \pm 0.53_{\text{stat}} \pm 0.42_{\text{sys}} \left(\begin{smallmatrix} +0.50 \\ -0.54 \end{smallmatrix} \right)_{\text{theory}}] \times 10^{-4}, \quad (\text{BELLE [33]}),$$

$$\mathcal{B}(b \rightarrow s\gamma) = (3.11 \pm 0.80_{\text{stat}} \pm 0.72_{\text{sys}}) \times 10^{-4}, \quad (\text{ALEPH [34]}),$$

in which full correlation of the “theory” errors has been assumed. The averages (27) and (28) are perfectly consistent with the SM predictions [35,36]

$$\mathcal{B}(\overline{\text{B}} \rightarrow X_s \gamma \ (E_\gamma > 1.6 \text{ GeV}))_{\text{SM}} = (3.57 \pm 0.30) \times 10^{-4}, \quad (29)$$

$$\mathcal{B}(\overline{\text{B}} \rightarrow X_s \gamma \ (E_\gamma > \frac{1}{20} m_b))_{\text{SM}} = 3.70 \times 10^{-4}. \quad (30)$$

By convention, contributions to $\overline{B} \rightarrow X_s \gamma$ from the intermediate real ψ and ψ' are treated as background, while all the continuum $c\bar{c}$ states are included assuming quark-hadron duality. Non-continuum states other than ψ and ψ' have negligible effect.

When the theoretical result (29) is reevaluated without use of the CKM unitarity in the dominant contributions (i.e. everywhere except for three small ($< 2.5\%$) corrections), comparison with the experiment (27) leads to the following constraint on the CKM matrix elements

$$|1.69 \lambda_u + 1.60 \lambda_c + 0.60 \lambda_t| = (0.94 \pm 0.07) |V_{cb}|. \quad (31)$$

After using the numerical values of $\lambda_c \simeq |V_{cb}| = (41.0 \pm 2.1) \times 10^{-3}$ and λ_u from the PDG [37], this equation yields $\lambda_t \simeq -47 \times 10^{-3}$ with an error of around 17%. This is consistent with the unitarity relation $\lambda_c \simeq -\lambda_t$. This relation, however, holds in the SM with much better accuracy than what has just been derived from Eq. (31). On the other hand, if the SM with 3 generations is not valid, Eq. (31) is not valid either.

Contrary to $\mathcal{B}(\overline{B} \rightarrow X_s \gamma)$, the branching ratio $\mathcal{B}(\overline{B} \rightarrow X_d \gamma)$, if measured, would provide us with useful constraints on the Wolfenstein parameters $\bar{\rho}$ and $\bar{\eta}$. After using the CKM unitarity, it can be written as

$$\mathcal{B}(\overline{B} \rightarrow X_d \gamma) = \frac{|\xi_t|^2}{|V_{cb}|^2} D_t + \frac{|\xi_u|^2}{|V_{cb}|^2} D_u + \frac{Re(\xi_t^* \xi_u)}{|V_{cb}|^2} D_r + \frac{Im(\xi_t^* \xi_u)}{|V_{cb}|^2} D_i. \quad (32)$$

The factors ξ_i have been defined earlier. The quantities D_a ($a = t, u, r, i$), which depend on various input parameters such as m_t, m_b, m_c, μ_b and α_s , are given in Ref. [38]. Typical values of these quantities (in units of λ^4) are: $D_t = 0.154$, $D_u = 0.012$, $D_r = -0.028$, and $D_i = 0.042$, corresponding to the scale $\mu = 5$ GeV, and the pole quark mass ratio $m_c/m_b = 0.29$. The charge-conjugate averaged branching ratio $\langle \mathcal{B}(B \rightarrow X_d \gamma) \rangle$ is obtained by discarding the last term on the right hand side of Eq. (32).

It is convenient to consider the ratio

$$\begin{aligned} \frac{\langle \mathcal{B}(B \rightarrow X_d \gamma) \rangle}{\langle \mathcal{B}(B \rightarrow X_s \gamma) \rangle} &= \frac{|\xi_t|^2}{|\lambda_t|^2} + \frac{D_u}{D_t} \frac{|\xi_u|^2}{|\lambda_t|^2} + \frac{D_r}{D_t} \frac{Re(\xi_t^* \xi_u)}{|\lambda_t|^2} \\ &= \lambda^2 \left[(1 - \bar{\rho})^2 + \bar{\eta}^2 + \frac{D_u}{D_t} (\bar{\rho}^2 + \bar{\eta}^2) + \frac{D_r}{D_t} (\bar{\rho}(1 - \bar{\rho}) - \bar{\eta}^2) \right] + O(\lambda^4) \\ &\simeq 0.036 \quad [\text{for } (\bar{\rho}, \bar{\eta}) = (0.22, 0.35)]. \end{aligned} \quad (33)$$

The above result together with Eq. (30) implies $\langle \mathcal{B}(B \rightarrow X_d \gamma) \rangle \simeq 1.3 \times 10^{-5}$ in the SM. Thus, with $O(10^8)$ $B\overline{B}$ events already collected at the B factories, $O(10^3)$ $b \rightarrow d\gamma$ decays are already produced. However, extracting them from the background remains a non-trivial issue.

Apart from the total branching ratios, the inclusive decays $\overline{B} \rightarrow X_{s(d)}\gamma$ provide us with other observables that might be useful for the CKM phenomenology. First, as discussed in Chapt. 3, the $\overline{B} \rightarrow X_s \gamma$ photon spectrum is used to extract the HQET parameters that are crucial for the determination of V_{ub} and $|V_{cb}|$. Second, CP-asymmetries contain information on the CKM phase. These asymmetries can be either direct (i.e. occur in the decay amplitudes) or induced by the $B\overline{B}$ mixing.

The mixing-induced CP-asymmetries in $\overline{B} \rightarrow X_{s(d)}\gamma$ are very small ($\mathcal{O}(m_{s(d)}/m_b)$) in the SM, so long as the photon polarizations are summed over. It follows from the particular structure of the dominant operator Q_7 in Eq. (25), which implies that photons produced in the decays of B and \overline{B} have opposite *circular* polarizations. Thus, in the absence of new physics, observation of the mixing-induced CP-violation would require selecting particular *linear* photon polarization with the help of matter-induced photon conversion into e^+e^- pairs [39].

The SM predictions for the direct CP-asymmetries read

$$\mathcal{A}_{\text{CP}}(B \rightarrow X_s \gamma) \equiv \frac{\Gamma(\overline{B} \rightarrow X_s \gamma) - \Gamma(B \rightarrow X_{\bar{s}} \gamma)}{\Gamma(\overline{B} \rightarrow X_s \gamma) + \Gamma(B \rightarrow X_{\bar{s}} \gamma)} \simeq \frac{\text{Im}(\lambda_t^* \lambda_u) D_i}{|\lambda_t|^2 D_t} \simeq 0.27 \lambda^2 \bar{\eta} \sim 0.5\%, \quad (34)$$

$$\mathcal{A}_{\text{CP}}(B \rightarrow X_d \gamma) \equiv \frac{\Gamma(\bar{B} \rightarrow X_d \gamma) - \Gamma(B \rightarrow X_{\bar{d}} \gamma)}{\Gamma(\bar{B} \rightarrow X_d \gamma) + \Gamma(B \rightarrow X_{\bar{d}} \gamma)} \simeq \frac{\text{Im}(\xi_t^* \xi_u) D_i}{|\xi_t|^2 D_t} \simeq \frac{-0.27 \bar{\eta}}{(1-\bar{\rho})^2 + \bar{\eta}^2} \sim -13\%, \quad (35)$$

where $\bar{\rho} = 0.22$ and $\bar{\eta} = 0.35$ have been used in the numerical estimates. As stressed in Ref. [38], there is considerable scale uncertainty in the above predictions, which would require a NLO calculation of D_i to be brought under theoretical control. The smallness of $\mathcal{A}_{\text{CP}}(B \rightarrow X_s \gamma)$ is caused by three suppression factors: λ_u/λ_t , α_s/π and m_c^2/m_b^2 . This SM prediction is consistent with the CLEO bound $-0.27 < \mathcal{A}_{\text{CP}}(B \rightarrow X_s \gamma) < +0.10$ at 95% C.L. [40].

No experimental limit has been announced so far on either the branching ratio $\mathcal{B}(\bar{B} \rightarrow X_d \gamma)$ or the CP asymmetry $\mathcal{A}_{\text{CP}}(B \rightarrow X_d \gamma)$. While experimentally challenging, the measurement of these quantities might ultimately be feasible at the B-factories which would provide valuable and complementary constraints on the CKM parameters.

2.2. Exclusive radiative B decays

The effective Hamiltonian sandwiched between the B-meson and a single meson state (say, K^* or ρ in the transitions $B \rightarrow (K^*, \rho)\gamma$) can be expressed in terms of matrix elements of bilinear quark currents inducing heavy-light transitions. These matrix elements are dominated by strong interactions at small momentum transfer and cannot be calculated perturbatively. They have to be obtained from a non-perturbative method, such as the lattice-QCD and the QCD sum rule approach. As the inclusive branching ratio $\mathcal{B}(B \rightarrow X_s \gamma)$ in the SM is in striking agreement with data, the role of the branching ratio $\mathcal{B}(B \rightarrow K^* \gamma)$ is that it will determine the form factor governing the electromagnetic penguin transition, $T_1^{K^*}(0)$.

To get a firmer theoretical prediction on the decay rate, one has to include the perturbative QCD radiative corrections arising from the vertex renormalization and the hard spectator interactions. To incorporate both types of QCD corrections, it is helpful to use a factorization Ansatz for the heavy-light transitions at large recoil and at leading order in the inverse heavy meson mass, introduced in Ref. [41]. Exemplified here by the $B \rightarrow V\gamma^*$ transition, a typical amplitude $f_k(q^2)$ can be written in the form

$$f_k(q^2) = C_{\perp k} \xi_{\perp}(q^2) + C_{\parallel k} \xi_{\parallel}(q^2) + \Phi_B \otimes T_k(q^2) \otimes \Phi_V, \quad (36)$$

where $\xi_{\perp}(q^2)$ and $\xi_{\parallel}(q^2)$ are the two independent form factors in these decays remaining in the heavy quark and large energy limit; $T_k(q^2)$ is a hard-scattering kernel calculated to $O(\alpha_s)$; Φ_B and Φ_V are the light-cone distribution amplitudes of the B- and vector-meson, respectively, the symbol \otimes denotes convolution with T_k , and $C_k = 1 + O(\alpha_s)$ are the hard vertex renormalization coefficients. In a number of papers [42–44], the factorization Ansatz of Eq. (36) is shown to hold in $O(\alpha_s)$, leading to the explicit $O(\alpha_s)$ corrections to the amplitudes $B \rightarrow V\gamma$ and $B \rightarrow V\ell^+\ell^-$.

Experiment	$\mathcal{B}_{\text{exp}}(B^0(\bar{B}^0) \rightarrow K^{*0}(\bar{K}^{*0}) + \gamma)$	$\mathcal{B}_{\text{exp}}(B^{\pm} \rightarrow K^{*\pm} + \gamma)$
CLEO [45]	$(4.55^{+0.72}_{-0.68} \pm 0.34) \times 10^{-5}$	$(3.76^{+0.89}_{-0.83} \pm 0.28) \times 10^{-5}$
BELLE [46]	$(3.91 \pm 0.23 \pm 0.25) \times 10^{-5}$	$(4.21 \pm 0.35 \pm 0.31) \times 10^{-5}$
BABAR [47]	$(4.23 \pm 0.40 \pm 0.22) \times 10^{-5}$	$(3.83 \pm 0.62 \pm 0.22) \times 10^{-5}$

Table 6.2: Experimental branching ratios for the decays $B^0(\bar{B}^0) \rightarrow K^{*0}(\bar{K}^{*0})\gamma$ and $B^{\pm} \rightarrow K^{*\pm}\gamma$.

We first discuss the exclusive decay $B \rightarrow K^* \gamma$, for which data from the CLEO, BABAR, and BELLE measurements are available and given in Table 6.2 for the charge conjugated averaged branching ratios. We note that the BELLE data alone has reached a statistical accuracy of better than 10%.

Adding the statistical and systematic errors in quadrature, we get the following world averages for the branching ratios:

$$\begin{aligned}\mathcal{B}(B^0 \rightarrow K^{*0}\gamma) &= (4.08 \pm 0.26) \times 10^{-5}, \\ \mathcal{B}(B^\pm \rightarrow K^\pm\gamma) &= (4.05 \pm 0.35) \times 10^{-5}.\end{aligned}\quad (37)$$

The two branching ratios are completely consistent with each other, ruling out any significant isospin breaking in the respective decay widths, which is not expected in the SM [48] but anticipated in some beyond-the-SM scenarios. Likewise, the CP asymmetry in $B \rightarrow K^*\gamma$ decays, which in the SM is expected to be of the same order of magnitude as for the inclusive decay, namely $\mathcal{A}_{\text{CP}}(B \rightarrow K^*\gamma) \leq 1\%$, is completely consistent with the present experimental bounds, the most stringent of which is posted by the BELLE collaboration [46]: $\mathcal{A}_{\text{CP}}(B \rightarrow K^*\gamma) = -0.022 \pm 0.048 \pm 0.017$. In view of this, we shall concentrate in the following on the branching ratios in $B \rightarrow K^*\gamma$ decays to determine the form factors.

Ignoring the isospin differences in the decay widths of $B \rightarrow K^*\gamma$ decays, the branching ratios for $B^\pm \rightarrow K^{*\pm}\gamma$ and $B^0(\bar{B}^0) \rightarrow K^{*0}(\bar{K}^{*0})\gamma$ can be expressed as:

$$\begin{aligned}\mathcal{B}_{\text{th}}(B \rightarrow K^*\gamma) &= \tau_B \Gamma_{\text{th}}(B \rightarrow K^*\gamma) \\ &= \tau_B \frac{G_F^2 \alpha |V_{tb} V_{ts}^*|^2}{32\pi^4} m_{b,\text{pole}}^2 M^3 \left[\xi_{\perp}^{(K^*)} \right]^2 \left(1 - \frac{M_{K^*}^2}{M^2} \right)^3 \left| C_7^{(0)\text{eff}} + A^{(1)}(\mu) \right|^2,\end{aligned}\quad (38)$$

where G_F is the Fermi coupling constant, $\alpha = \alpha(0) = 1/137$ is the fine-structure constant, $m_{b,\text{pole}}$ is the pole b -quark mass, M and M_{K^*} are the B - and K^* -meson masses, and τ_B is the lifetime of the B^0 - or B^+ -meson. The quantity $\xi_{\perp}^{(K^*)}$ is the soft part of the form factor $T_1^{K^*}(q^2 = 0)$ in the $B \rightarrow K^*\gamma$ transition, to which the symmetries in the large energy limit apply. The two form factors $\xi_{\perp}^{(K^*)}$ and $T_1^{K^*}(q^2 = 0)$ are related by perturbative ($O(\alpha_s)$) and power ($O(\Lambda_{\text{QCD}}/m_b)$) corrections [50]. Thus, one could have equivalently expressed the $O(\alpha_s)$ -corrected branching ratio for $B \rightarrow K^*\gamma$ in terms of the QCD form factor $T_1^{K^*}(q^2 = 0)$, and a commensurately modified expression for the explicit $O(\alpha_s)$ correction in the above equation [43]. In any case, the form factor $T_1^{K^*}(q^2 = 0)$ or $\xi_{\perp}^{(K^*)}$ has to be determined by a non-perturbative method.

The function $A^{(1)}$ in Eq. (38) can be decomposed into the following three components:

$$A^{(1)}(\mu) = A_{C_7}^{(1)}(\mu) + A_{\text{ver}}^{(1)}(\mu) + A_{\text{sp}}^{(1)K^*}(\mu_{\text{sp}}). \quad (39)$$

Here, $A_{C_7}^{(1)}$ and $A_{\text{ver}}^{(1)}$ are the $O(\alpha_s)$ (i.e. NLO) corrections due to the Wilson coefficient C_7^{eff} and in the $b \rightarrow s\gamma$ vertex, respectively, and $A_{\text{sp}}^{(1)K^*}$ is the $\mathcal{O}(\alpha_s)$ hard-spectator correction to the $B \rightarrow K^*\gamma$ amplitude computed in [42–44]. This formalism leads to the following branching ratio for $B \rightarrow K^*\gamma$ decays:

$$\mathcal{B}_{\text{th}}(B \rightarrow K^*\gamma) \simeq (7.2 \pm 1.1) \times 10^{-5} \left(\frac{\tau_B}{1.6 \text{ ps}} \right) \left(\frac{m_{b,\text{pole}}}{4.65 \text{ GeV}} \right)^2 \left(\frac{\xi_{\perp}^{(K^*)}}{0.35} \right)^2, \quad (40)$$

where the default values of the three input parameters are made explicit, with the rest of the theoretical uncertainties indicated numerically; the default value for the form factor $\xi_{\perp}^{(K^*)}(0)$ is based on the light-cone QCD sum rule estimates [49].

The non-perturbative parameter $\xi_{\perp}^{(K^*)}(0)$ can now be extracted from the data on the branching ratios for $B \rightarrow K^*\gamma$ decays, given in Eq. (37), leading to the current world average $\langle \mathcal{B}(B \rightarrow K^*\gamma) \rangle = (4.06 \pm 0.21) \times 10^{-5}$, which then yields

$$\bar{\xi}_{\perp}^{(K^*)}(0) = 0.25 \pm 0.04, \quad \left[\bar{T}_1^{(K^*)}(0, \bar{m}_b) = 0.27 \pm 0.04 \right], \quad (41)$$

where we have used the $O(\alpha_s)$ relation between the effective theory form factor $\xi_\perp^{(K^*)}(0)$ and the full QCD form factor $T_1^{(K^*)}(0, \bar{m}_b)$, worked out in [50]. This estimate is significantly smaller than the corresponding predictions from the QCD sum rules analysis $T_1^{(K^*)}(0) = 0.38 \pm 0.06$ [51,49] and from the lattice simulations $T_1^{(K^*)}(0) = 0.32^{+0.04}_{-0.02}$ [52]. Clearly, more work is needed to calculate the $B \rightarrow K^*\gamma$ decay form factors precisely.

As already discussed, inclusive $b \rightarrow d\gamma$ transitions are not yet available experimentally. This lends great importance to the exclusive decays, such as $B \rightarrow \rho\gamma, \omega\gamma$, to whose discussion we now turn. These decays differ from their $B \rightarrow K^*\gamma$ counterparts, in that the annihilation contributions are not Cabibbo-suppressed. In particular, the isospin-violating ratios and CP-asymmetries in the decay rates involving the decays $B^\pm \rightarrow \rho^\pm\gamma$ and $B^0(\bar{B}^0) \rightarrow \rho^0\gamma$ are sensitive to the penguin and annihilation interference in the amplitudes.

We recall that ignoring the perturbative QCD corrections to the penguin amplitudes the ratio of the branching ratios for the charged and neutral B-meson decays in $B \rightarrow \rho\gamma$ can be written as [53,54]

$$\frac{\mathcal{B}(B^- \rightarrow \rho^-\gamma)}{2\mathcal{B}(B^0 \rightarrow \rho^0\gamma)} \simeq \left| 1 + \epsilon_A e^{i\phi_A} \frac{V_{ub}V_{ud}^*}{V_{tb}V_{td}^*} \right|^2, \quad (42)$$

where $\epsilon_A e^{i\phi_A}$ includes the dominant W -annihilation and possible sub-dominant long-distance contributions. We shall use the value $\epsilon_A \simeq +0.30 \pm 0.07$ for the decays $B^\pm \rightarrow \rho^\pm\gamma$ [55,56], obtained assuming factorization of the annihilation amplitude. The corresponding quantity for the decays $B^0 \rightarrow \rho^0\gamma$ is suppressed due to the electric charge of the spectator quark in B^0 as well as by the unfavourable colour factors. Typical estimates for ϵ_A in $B^0 \rightarrow \rho^0\gamma$ put it at around 5% [55,56]. The strong interaction phase ϕ_A vanishes in $\mathcal{O}(\alpha_s)$ in the chiral limit and to leading twist [54], giving theoretical credibility to the factorization-based estimates. Thus, in the QCD factorization approach the phase ϕ_A is expected to be small and one usually sets $\phi_A = 0$. Of course, $O(\alpha_s)$ vertex and hard spectator corrections generate non-zero strong phases, as discussed later. The isospin-violating correction depends on the unitarity triangle phase α due to the relation:

$$\frac{V_{ub}V_{ud}^*}{V_{tb}V_{td}^*} = - \left| \frac{V_{ub}V_{ud}^*}{V_{tb}V_{td}^*} \right| e^{i\alpha}. \quad (43)$$

The NLO corrections to the branching ratios of the exclusive decays $B^\pm \rightarrow \rho^\pm\gamma$ and $B^0 \rightarrow \rho^0\gamma$ are derived very much along the same lines as outlined for the decays $B \rightarrow K^*\gamma$. Including the annihilation contribution, the $B \rightarrow \rho\gamma$ branching ratios, isospin- and CP-violating asymmetries are given in [43,44].

Concentrating on the decays $B^\pm \rightarrow \rho^\pm\gamma$, the expression for the ratio $R(\rho\gamma/K^*\gamma) \equiv \mathcal{B}(B^\pm \rightarrow \rho^\pm\gamma)/\mathcal{B}(B^\pm \rightarrow K^{*\pm}\gamma)$ (where an average over the charge-conjugated modes is implied) can be written as [44]

$$R(\rho\gamma/K^*\gamma) = S_\rho \left| \frac{V_{td}}{V_{ts}} \right|^2 \frac{(M_B^2 - M_\rho^2)^3}{(M_B^2 - M_{K^*}^2)^3} \zeta^2 (1 + \Delta R), \quad (44)$$

where $S_\rho = 1$ for the ρ^\pm meson, and $\zeta = \xi_\perp^\rho(0)/\xi_\perp^{K^*}(0)$, with $\xi_\perp^\rho(0)(\xi_\perp^{K^*}(0))$ being the form factors (at $q^2 = 0$) in the effective heavy quark theory for the decays $B \rightarrow \rho\gamma$ ($B \rightarrow K^*\gamma$). The quantity $(1 + \Delta R)$ entails the explicit $O(\alpha_s)$ corrections, encoded through the functions $A_R^{(1)K^*}$, $A_R^{(1)t}$ and A_R^u , and the long-distance contribution L_R^u . For the decays $B^\pm \rightarrow \rho^\pm\gamma$ and $B^\pm \rightarrow K^{*\pm}\gamma$, this can be written after charge conjugated averaging as

$$\begin{aligned} 1 + \Delta R^\pm &= \left| \frac{C_7^d + \lambda_u L_R^u}{C_7^s} \right|^2 \left(1 - 2A_R^{(1)K^*} \frac{\Re C_7^s}{|C_7^s|^2} \right) \\ &\quad + \frac{2}{|C_7^s|^2} \Re \left[(C_7^d + \lambda_u L_R^u)(A_R^{(1)t} + \lambda_u^* A_R^u) \right]. \end{aligned} \quad (45)$$

$\zeta = 0.76 \pm 0.10$	$L_R^u = -0.095 \pm 0.022$
$A^{(1)K^*} = -0.113 - i0.043$	$A^{(1)t} = -0.114 - i0.045$
$A^u = -0.0181 + i0.0211$	
$\eta_{tt} = 0.57$	$\eta_{cc} = 1.38 \pm 0.53$
$\eta_{tc} = 0.47 \pm 0.04$	$\hat{B}_K = 0.86 \pm 0.15$
$\eta_B = 0.55$	$F_{B_d} \sqrt{\hat{B}_{B_d}} = 235 \pm 33^{+0}_{-24} \text{ MeV}$
$\xi_s = 1.18 \pm 0.04^{+0.12}_{-0}$	
$\lambda = 0.221 \pm 0.002$	$ V_{ub}/V_{cb} = 0.097 \pm 0.010$
$\epsilon_K = (2.271 \pm 0.017) 10^{-3}$	$\Delta M_{B_d} = 0.503 \pm 0.006 \text{ ps}^{-1}$
$a_{\psi K_s} = 0.734 \pm 0.054$	$\Delta M_{B_s} \geq 14.4 \text{ ps}^{-1} (95\% \text{ C.L.})$

Table 6.3: *Theoretical parameters and measurements used in $B \rightarrow \rho\gamma$ observables and in the CKM unitarity fits. For details and references, see [57,17]*

In the SM, $C_7^d = C_7$, as in the $b \rightarrow s\gamma$ decays; however, in beyond-the-SM scenarios, this may not hold making the decays $B \rightarrow \rho\gamma$ interesting for beyond-the-SM searches [57]. The definitions of the quantities $A^{(1)K^*}$, $A^{(1)t}$, A^u and $L_R^u = \epsilon_A C_7^{(0)\text{eff}}$ can be seen in [44]. Their default values together with that of ζ are summarized in Table 6.3, where we have also specified the theoretical errors in the more sensitive parameters ζ and L_R^u .

What concerns the quantity called ζ , we note that there are several model-dependent estimates of the same in the literature. Some representative values are: $\zeta = 0.76 \pm 0.06$ from the light-cone QCD sum rules [55]; a theoretically improved estimate in the same approach yields [49]: $\zeta = 0.75 \pm 0.07$; $\zeta = 0.88 \pm 0.02(1)$ using hybrid QCD sum rules [58], and $\zeta = 0.69 \pm 10\%$ in the quark model [59]. Except for the hybrid QCD sum rules, all other approaches yield a significant SU(3)-breaking in the magnetic moment form factors. In the light-cone QCD sum rule approach, this is anticipated due to the appreciable differences in the wave functions of the K^* and ρ -mesons. To reflect the current dispersion in the theoretical estimates of ζ , we take its value as $\zeta = 0.76 \pm 0.10$. A lattice-QCD based estimate of the same is highly desirable.

The isospin breaking ratio

$$\Delta(\rho\gamma) \equiv \frac{(\Delta^{+0} + \Delta^{-0})}{2}, \quad \Delta^{\pm 0} = \frac{\Gamma(B^\pm \rightarrow \rho^\pm \gamma)}{2\Gamma(B^0(\bar{B}^0) \rightarrow \rho^0 \gamma)} - 1 \quad (46)$$

is given by

$$\begin{aligned} \Delta(\rho\gamma) &= \left| \frac{C_7^d + \lambda_u L_R^u}{C_7^d} \right|^2 \left(1 - \frac{2\Re C_7^d (A_R^{(1)t} + \lambda_u^* A_R^u)}{|C_7^d|^2} \right) \\ &+ \frac{2}{|C_7^d|^2} \Re \left[(C_7^d + \lambda_u L_R^u) (A_R^{(1)t} + \lambda_u^* A_R^u) \right] - 1, \end{aligned} \quad (47)$$

and the CP asymmetry $A_{CP}^\pm(\rho\gamma) = (\mathcal{B}(B^- \rightarrow \rho^-\gamma) - \mathcal{B}(B^+ \rightarrow \rho^+\gamma)) / (\mathcal{B}(B^- \rightarrow \rho^-\gamma) + \mathcal{B}(B^+ \rightarrow \rho^+\gamma))$ is

$$A_{CP}^\pm(\rho\gamma) = -\frac{2\Im \left[(C_7^d + \lambda_u L_R^u) (A_I^{(1)t} + \lambda_u^* A_I^u) \right]}{|C_7^d + \lambda_u L_R^u|^2}. \quad (48)$$

The observables $R^0(\rho\gamma/K^*\gamma) \equiv \bar{\mathcal{B}}(B^0 \rightarrow \rho^0\gamma) / \mathcal{B}(\bar{B}^0 \rightarrow K^{*0}\gamma)$ (where $\bar{\mathcal{B}}$ is the average of the B^0 and \bar{B}^0 modes) and $A_{CP}^0(\rho\gamma) = (\mathcal{B}(B^0 \rightarrow \rho^0\gamma) - \mathcal{B}(\bar{B}^0 \rightarrow \rho^0\gamma)) / (\mathcal{B}(B^0 \rightarrow \rho^0\gamma) + \mathcal{B}(\bar{B}^0 \rightarrow \rho^0\gamma))$ are

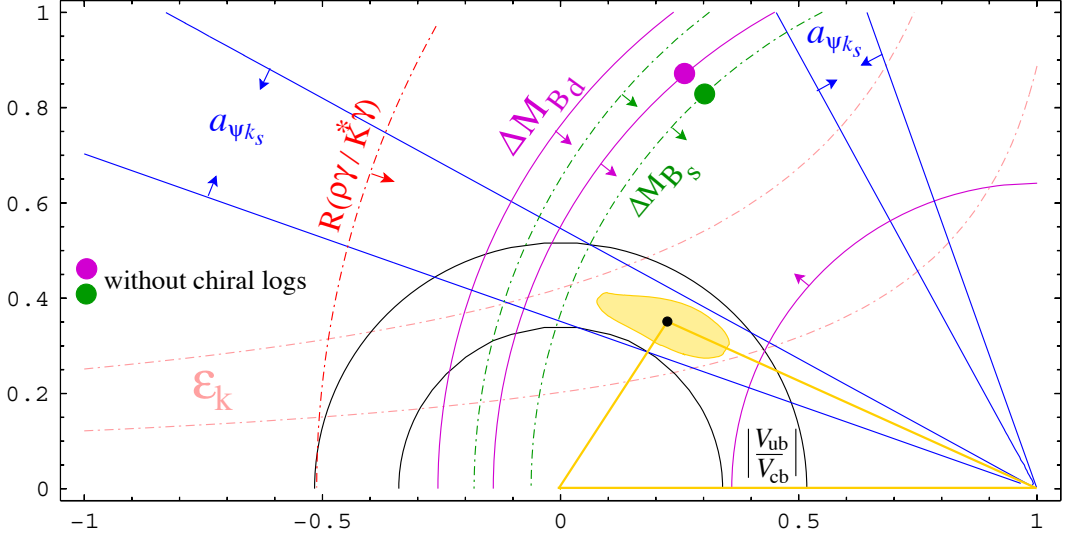


Fig. 6.10: Unitary triangle fit in the SM and the resulting 95% C.L. contour in the $\bar{\rho}$ - $\bar{\eta}$ plane. The impact of the $R(\rho\gamma/K^*\gamma) < 0.047$ constraint is also shown (from Ref. [57]).

obtained from Eqs. (44, 45, 48) in the limit $L_R^u = 0$ and $S_\rho = 1/2$. The numerical estimates for the various observables depend, apart from the hadronic parameters specific to the $B \rightarrow V\gamma$ ($V = K^*, \rho$) decays, also on the CKM parameters, in particular $\bar{\rho}$ and $\bar{\eta}$. A typical analysis of the constraints in the $(\bar{\rho}, \bar{\eta})$ plane from the unitarity of the CKM matrix [57], including the measurements of the CP asymmetry $a_{\psi K_s}$ in the decays $B^0/\bar{B}^0 \rightarrow J/\psi K_s$ (and related modes) [60] is shown in Fig. 6.10. Note that for the hadronic parameters $F_{B_d}\sqrt{\hat{B}_{B_d}}$ and ξ_s , the recent lattice estimates [61] have been adopted that take into account uncertainties induced by the so-called chiral logarithms [62]. These errors are extremely asymmetric and, once taken into account, reduce sizeably the impact of the $\Delta M_{B_s}/\Delta M_{B_d}$ lower bound on the unitarity triangle analysis, as shown in Fig. 6.10. The 95% CL contour is drawn taking into account chiral logarithms uncertainties. The fitted values for the Wolfenstein parameters are $\bar{\rho} = 0.22 \pm 0.07$ and $\bar{\eta} = 0.35 \pm 0.04$. This yields $\Delta R^\pm = 0.055 \pm 0.130$ and $\Delta R^0 = 0.015 \pm 0.110$ [44,57]. The impact of the current upper limit $R(\rho\gamma/K^*\gamma) \leq 0.047$ [63] is also shown. While not yet competitive to the existing constraints on the unitarity triangle, this surely is bound to change with the anticipated $O(1 \text{ (ab)}^{-1})$ $\Upsilon(4S) \rightarrow B\bar{B}$ data over the next three years at the B-factories.

Taking into account these errors and the uncertainties on the theoretical parameters presented in Table 6.3, leads to the following SM expectations for the $B \rightarrow (K^*, \rho)\gamma$ decays [57]:

$$R^\pm(\rho\gamma/K^*\gamma) = 0.023 \pm 0.012 , \quad (49)$$

$$R^0(\rho\gamma/K^*\gamma) = 0.011 \pm 0.006 , \quad (50)$$

$$\Delta(\rho\gamma) = 0.04^{+0.14}_{-0.07} , \quad (51)$$

$$A_{CP}^\pm(\rho\gamma) = 0.10^{+0.03}_{-0.02} , \quad (52)$$

$$A_{CP}^0(\rho\gamma) = 0.06 \pm 0.02 . \quad (53)$$

The above estimates of $R^\pm(\rho\gamma/K^*\gamma)$ and $R^0(\rho\gamma/K^*\gamma)$ can be combined with the measured branching ratios for $B \rightarrow K^*\gamma$ decays given earlier to yield:

$$\mathcal{B}(B^\pm \rightarrow \rho^\pm \gamma) = (0.93 \pm 0.49) \times 10^{-6} , \quad \mathcal{B}(B^0 \rightarrow \rho^0 \gamma) = (0.45 \pm 0.24) \times 10^{-6} . \quad (54)$$

The errors include the uncertainties on the hadronic parameters and the CKM parameters $\bar{\rho}$, $\bar{\eta}$, as well as the current experimental error on $\mathcal{B}(B \rightarrow K^*\gamma)$. While there is as yet no experimental bounds

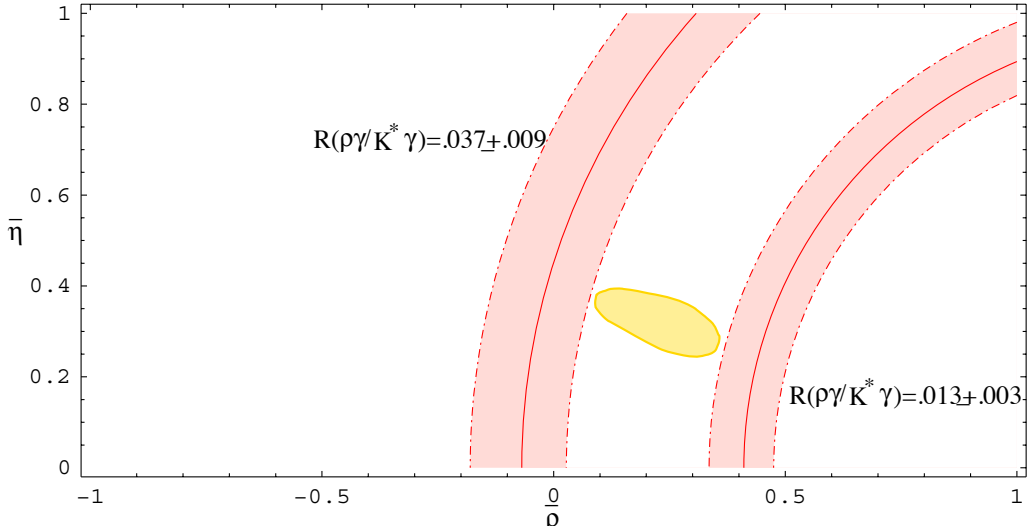


Fig. 6.11: Extremal values of $R(\rho\gamma/K^*\gamma)$ that are compatible with the SM unitarity triangle analysis (from Ref. [57]).

on the isospin- and CP-violating quantities, $\Delta(\rho\gamma)$, $A_{CP}^\pm(\rho\gamma)$ and $A_{CP}^0(\rho\gamma)$, the upper limits on the branching ratios $R^\pm(\rho\gamma/K^*\gamma)$ and $R^0(\rho\gamma/K^*\gamma)$ have been significantly improved by the BABAR [63] and BELLE [46] collaborations recently. Averaged over the charge conjugated modes, the current best upper limits are [63]: $\mathcal{B}(B^0 \rightarrow \rho^0\gamma) < 1.4 \times 10^{-6}$, $\mathcal{B}(B^\pm \rightarrow \rho^\pm\gamma) < 2.3 \times 10^{-6}$ and $\mathcal{B}(B^0 \rightarrow \omega\gamma) < 1.2 \times 10^{-6}$ (at 90% C.L.). They have been combined, using isospin weights for $B \rightarrow \rho\gamma$ decays and assuming $\mathcal{B}(B^0 \rightarrow \omega\gamma) = \mathcal{B}(B^0 \rightarrow \rho^0\gamma)$, to yield the improved upper limit $\mathcal{B}(B \rightarrow \rho\gamma) < 1.9 \times 10^{-6}$. The current measurements of the branching ratios for $B \rightarrow K^*\gamma$ decays by BABAR [47], $\mathcal{B}(B^0 \rightarrow K^{*0}\gamma) = (4.23 \pm 0.40 \pm 0.22) \times 10^{-5}$ and $\mathcal{B}(B^+ \rightarrow K^{*+}\gamma) = (3.83 \pm 0.62 \pm 0.22) \times 10^{-5}$, are then used to set an upper limit on the ratio of the branching ratios $R(\rho\gamma/K^*\gamma) \equiv \mathcal{B}(B \rightarrow \rho\gamma)/\mathcal{B}(B \rightarrow K^*\gamma) < 0.047$ (at 90% C.L.) [63]. This bound is typically a factor 2 away from the SM estimates given above [44,57]. However, in beyond-the-SM scenarios, this bound provides highly significant constraints on the relative strengths of the $b \rightarrow d\gamma$ and $b \rightarrow s\gamma$ transitions [57].

The extremal values of $R(\rho\gamma/K^*\gamma)$ compatible with the SM UT-analysis are shown in Fig. 6.11 where the bands correspond to the values 0.037 ± 0.007 and 0.013 ± 0.003 (the errors are essentially driven by the uncertainty on ζ). The meaning of this figure is as follows: any measurement of $R(\rho\gamma/K^*\gamma)$, whose central value lies in the range $(0.013, 0.037)$ would be compatible with the SM, irrespective of the size of the experimental error. The error induced by the imprecise determination of the isospin breaking parameter ζ limits currently the possibility of having a very sharp impact from $R(\rho\gamma/K^*\gamma)$ on the UT analysis. This aspect needs further theoretical work.

3. Weak phases from hadronic B decays

M. Beneke, G. Buchalla (coordinator), M. Ciuchini, R. Fleischer, E. Franco, Y.-Y. Keum, G. Martinelli, M. Pierini, J.L. Rosner and L. Silvestrini

The next five contributions discuss the problem of extracting weak phases from hadronic B decays. The emphasis is on determining the CKM parameters γ and α , or equivalent constraints on $\bar{\rho}$ and $\bar{\eta}$, from exclusive modes with two light mesons in the final state, such as $B \rightarrow \pi K$ and $B \rightarrow \pi\pi$. This problem is difficult since the underlying weak interaction processes are dressed by QCD dynamics, which is prominent in purely hadronic decays. Despite the general difficulty, there are several circumstances that help us to control strong interaction effects and to isolate the weak couplings: